ICNMM2020-1041

EVOLUTION OF HEAT TRANSFER IN POOL BOILING IN CONTAMINATED WATER

Jacob Graham¹, Angelo Hawa¹, Patricia Weisensee¹

¹Washington University in St. Louis, St. Louis, MO

ABSTRACT

Boiling heat transfer serves as an efficient mechanism to dissipate large amounts of thermal energy due to the latent heat of phase change. In academic studies, typically ultra-pure deionized (DI) water is used to avoid contamination. However, in industrial and commercial settings, the working fluid might be contaminated with sediments, dust, salts, or organic matter. Long-term boiling processes in non-DI water cause substantial build-up of a stable layer of deposit that dramatically reduces the heat transfer coefficient. Therefore, heating applications in a contaminated medium demand strategies to prevent such fouling. Here, we studied the use of lubricant infused surfaces (LIS) and their ability to possibly minimize the deposition of calcium sulfate. Aluminum samples were infused with Krytox 102 oil and the heat transfer coefficient was investigated at a vertical and horizontal surface orientation. Fouling effects were introduced by pool boiling for 7.5 hours in a 6.97 mM calcium sulfate solution at constant heat flux. Heat flux curves for both plain aluminum and LIS were calibrated before contamination. Initially, the LIS was unable to support a nucleate phase and transitioned directly from liquid convection to film boiling heat transfer. Upon partial degradation of the lubricant layer during long-run experiments, nucleate boiling ensued. Over 7.5 hours, the heat transfer coefficient of each sample (Al and LIS) degraded between 5.4% and 7.9% with no significant correlation with either lubricant treatment or surface orientation. Post boiling profilometry was conducted on each sample to characterize the thickness and distribution of the calcium sulfate layer. In these experiments, the plain aluminum surface outperformed the LIS at both orientations in minimizing calcium layer thickness. The LIS oriented vertically outperformed the LIS oriented horizontally.

Keywords: pool boiling, lubricant-infused surface, LIS, salt, fouling, deposition

NOMENCLATURE

heat transfer coefficient (kW/m²K) h thermal conductivity (W/m.K) k

heat flux (kW/m²)

 $T_{\text{sat}} \\$ saturation temperature of water (°C)

wall temperature (°C) T_{wall}

position (m) Х

area of copper heating stem (m²) A_{c} area of boiling surface (m²) A_s

1. INTRODUCTION

Cooling through latent heat of phase change is the most effective thermal management mechanism of industrial processes that produce excessive amounts of heat. During boiling heat transfer, a heated surface is submerged in a pool of liquid maintained at its saturation temperature to accelerate the process of vaporization and bubble departure. At the critical heat flux, an insulating layer of vapor forms over the surface, reverting the main heat transfer mechanism from nucleation and convection to conduction through the low-conductivity vapor film. Surpassing this heat flux causes a dramatic spike in heater temperature, which can cause catastrophic equipment failure. Because of these severe repercussions, heater systems often operate at much lower and less efficient heat fluxes. Therefore, developing mechanisms to increase both the critical heat flux and the boiling heat transfer coefficient of surfaces is the primary focus of active research this field.

Usage of contaminated coolant in power generation, desalination processes, and marine environments calls for strategies to mitigate scaling and (bio-) fouling during boiling. Contaminated water introduces a number of factors that influence the boiling heat transfer efficiency, including surface roughening and insulating effects. Surface roughening caused by incremental scaling increases the heat transfer efficiency by increasing the effective surface area and introducing capillary wicking¹. However, inevitable thickening of the fouling layer produces an insulating effect due to its low thermal conductivity². Deposition of salts such as calcium sulfate is particularly difficult to prevent during boiling as their solubility decreases with temperature, so particles have a higher propensity to precipitate out close to the superheated surface. Hydrophobic titania-fluoroalkylsilane (TiO2-FPS) coatings have been shown to reduce calcium sulfate deposition rates on stainless steel surfaces³. Additionally, ion implantation and electron sputtering have been proven as effective anti-fouling mechanisms in the presence of CaSO₄⁴. In this paper, we study the impacts of infusing lubricant onto a nanoporous aluminum surface coated with a superhydrophobic layer of hexadecyltrimethoxysilane (HTMS) on the critical heat flux (CHF) and the boiling heat transfer coefficient (BHTC). Lubricant infused surfaces (LIS) are easy and economical to fabricate, scalable, and selfhealing^{5,6}. LIS have shown to be excellent candidates to improve the efficiency of condensation heat transfer^{7,8}, and to mitigate (bio-)fouling and even mussel attack in marine environments^{9,10}. Here, we hypothesized that LIS can also prevent precipitate from settling on the surface during pool boiling. To test our hypothesis, we monitored the evolution of the BHTC at both horizontal and vertical orientations on plain aluminum and LIS over a duration of 7.5 hours. We characterized the thickness and distribution of the calcium sulfate layer using profilometry to determine the effects of the lubricant treatment and the surface orientation. Surprisingly, the salt built-up on LIS exceeded that of the bare aluminum, irrespective of the sample orientation. The reason for this apparent contradiction is yet to be determined.

2. MATERIALS AND METHODS

2.1 Sample Preparation

Six disk shaped aluminum test samples with a diameter of 25.4 mm and a thickness of 2.032 mm were machined with a 0.5 mm hole through the disk's side for a type-K thermocouple to be positioned 0.762 mm below the sample surface. Plain aluminum samples were rinsed with acetone, isopropanol, and DI water. They were dried with nitrogen gas and then cleaned in an oxygen plasma for 2 minutes (Plasma Preen II. Plasmatic Systems Inc.). Three samples were placed in DI water held at 95-98°C to produce a nanoporous boehmite layer on the sample surface. The samples were dried using nitrogen and placed in the plasma cleaner for 1 minute to activate the boehmite layer. The samples were subsequently placed alongside a mixture of 0.3 ml heptadecafluorodecyl-trimethoxy-silane (HTMS) Aldrich) and 2.7 ml Toluene in a covered petri dish in a furnace at 95°C for 4 hours to produce a thin HTMS coating to render the surface superhydrophobic. The samples were then spin coated using Krytox 102 oil (purchased from zoro.com) for 60s at 3500 RPM to prepare the lubricant infused surfaces.

2.2 Solution Preparation

A 6.97 mM solution of calcium sulfate was produced by magnetically mixing a fine calcium sulfate powder (Drierite, Sigma Aldrich) into DI water for approximately 48 hours. At 100°C, this solution has a concentration of 75% relative to saturation.

2.3 Apparatus

A 6x6 inch aluminum vacuum chamber (IdealVac) was custom-designed to measure the heat flux to a sample in a saturated medium during pool boiling, as shown in Fig. 1.

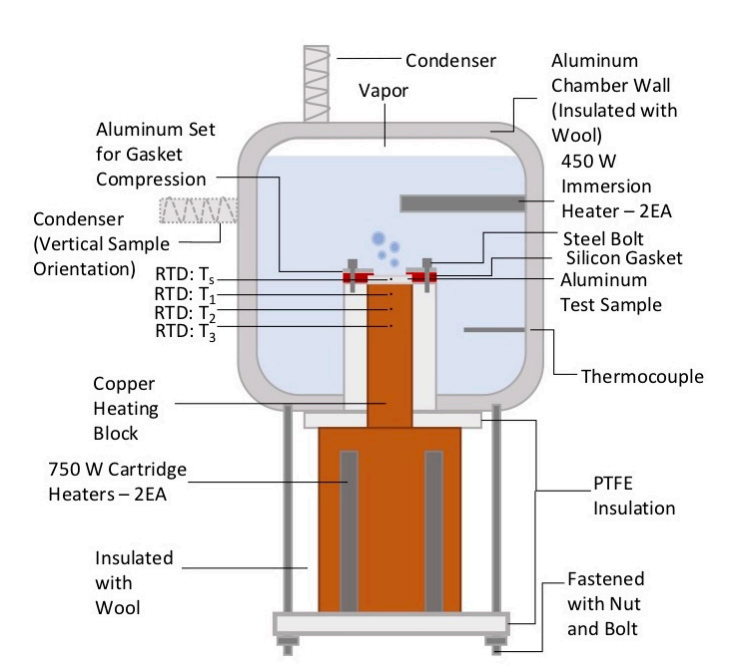


FIGURE 1: Schematic of the boiling chamber.

The chamber was wrapped in wool insulation to minimize heat losses from the pool. The pool temperature was monitored using a type-K thermocouple and maintained as closely to the saturation temperature $T_{\text{sat}} = 100^{\circ}\text{C}$ as possible using two 450watt immersion heaters (OEM Heaters). A condenser was mounted at the top of the chamber to maintain a consistent water level and calcium sulfate concentration. The chamber was fitted with an additional stem on the side to attach a condenser when the chamber was rotated for experiments in a vertical orientation. The chamber was open to the atmosphere through the condenser to maintain a constant pressure in the system. Two 750-watt cartridge heaters (Chromalox) were embedded in a cylindrical copper heating block (thermal conductivity $k_c \approx 390$ W/m.K; diameter $D_c = 7.62$ cm), which was insulated with fiberglass. Heat flow was directed through a 2.54 cm diameter stem protruding from the heating block. The stem was insulated using polytetrafluoroethylene (PTFE). Due to the low thermal conductivity of PTFE we approximate the heat flow through the stem as 1D. Holes were bored horizontally into the side of the stem to accommodate three 2 mm dia. embedment RTDs (MOD-TRONIC) at 1 cm intervals, which were fixed using a conductive curing silver paste. The test samples were mounted to the copper heating block using a non-curing conductive silver grease. A circular silicon gasket was compressed around the edges of the test samples using an aluminum set piece that was bolted into the PTFE insulating block, insuring good thermal contact and leaving a 1.5 cm diameter circular surface exposed for boiling.

2.4 Data analysis

Temperature data from the RTDs and thermocouples was collected at a sampling rate of 14.29 Hz using the NI cDAQ 9174 (National Instruments) interfaced with Matlab. The heat flux q was calculated using Fourier's Law in 1D:

$$q'' = \frac{q}{A_c} = k_c \frac{dT}{dx},\tag{1}$$

where q is the heat supplied by the cartridge heaters and A_c is the cross-sectional area of the copper stem. The temperature gradient through the copper stem was determined using the three point backward Taylor's series approximation:

$$\frac{dT}{dx} = \frac{3T_1 - 4T_2 + T_3}{2\Delta x},$$
 (2) where T_i are the temperature read-outs of the three RTDs

where T_i are the temperature read-outs of the three RTDs embedded in the copper stem, and Δx is the distance between each RTD. The sample surface temperature, or wall temperature T_{wall} , was extrapolated using the calculated heat flux and the temperature T_s from the RTD embedded in the sample. The boiling heat transfer coefficient h was calculated from Newton's Law of Cooling and the exposed area A_s of the boiling surface:

$$q = hA_s(T_{wall} - T_{sat}). (3)$$

3. RESULTS AND DISCUSSION

Initial critical heat flux curves were calibrated for both the plain aluminum surface and the LIS in DI water. The water reservoir was brought to its saturation temperature and degassed for 40 minutes via rigorous boiling. To measure the heat transfer performance of the different samples, the power supply connected to the embedded cartridge heaters was increased by 15 W every 5 minutes to define a consistent ramp rate. For the plain aluminum surface, nucleate boiling began at a superheat of 10.2 K. The CHF was observed at a surface superheat of approximately 29.3 K and a heat flux of $\approx 2350 \text{ kW/m}^2$, as seen in Fig. 2. For LIS, the boiling curve begins with an approximately linear increase in heat flux with superheat before boiling ensues. This linear phase is followed by a brief transition region when the first bubble forms and grows, after which the primary heat transfer mechanism becomes film boiling for ΔT > 10 K. Onset of nucleate boiling for the LIS occurred at a superheat of 7.6 K, however, the LIS was not able to sustain a nucleate boiling phase. The first bubble did not depart until it covered the entire sample surface, likely due to the mild hydrophobicity of the Krytox oil. This non-departure of the bubble resulted in a film boiling phase for most of the heat transfer curve shown in Fig 2. The lubricant infused surface supported a heat flux of only 142.7 kW/m² before it transitioned to film boiling.

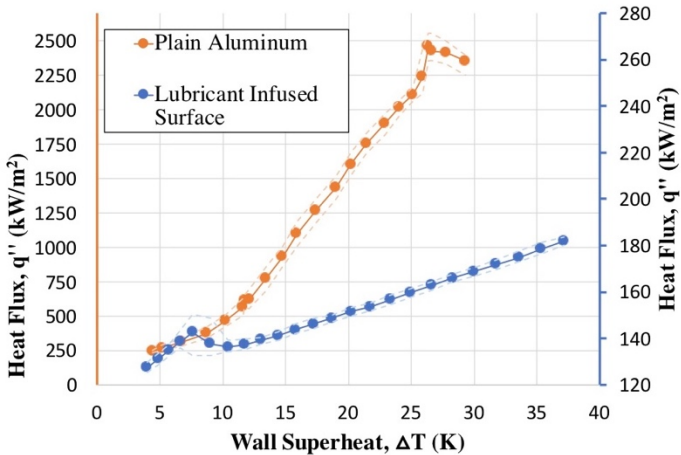


FIGURE 2: Critical heat flux curves for plain aluminum and LIS in DI water. Error lines show maximum and minimum heat fluxes measured during the sampling period of each data point. Note the different order of magnitude for plain aluminum (left axis) and LIS (right axis).

Fresh samples were prepared for experiments to capture heat transfer coefficient degradation in a 6.97 mM solution of CaSO₄. Evolution of the BHTC for plain aluminum and LIS oriented horizontally and vertically was tested over a 7.5-hour period. Heat fluxes were chosen to set an initial surface superheat of 18 K, based on the heat flux curve for the horizontally oriented samples. Based on Fig. 2, the LIS would support a much lower heat flux at this level of superheat. The initial heat flux, therefore, was set to 1050 kW/m² for the plain aluminum samples, while the heat flux for the LIS was set to 150 kW/m². In each experiment, after the surface temperature was allowed to stabilize, the heat transfer coefficient was averaged over 10-minute intervals for 7.5 hours. Figure 3 shows the evolution of the BHTC over this time period, normalized by the initial 10-minute average BHTC.

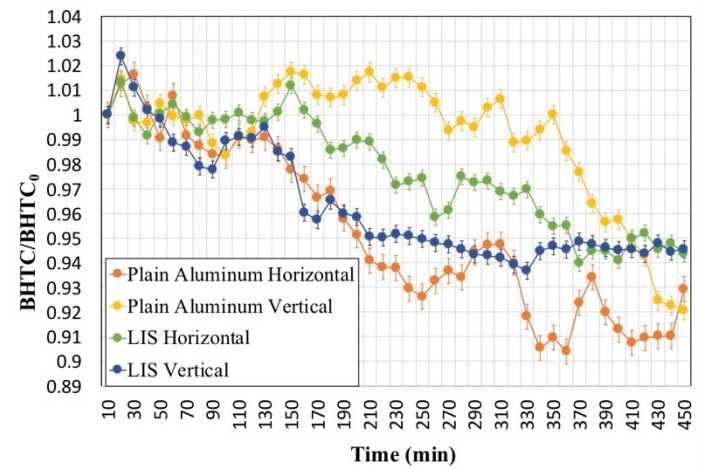
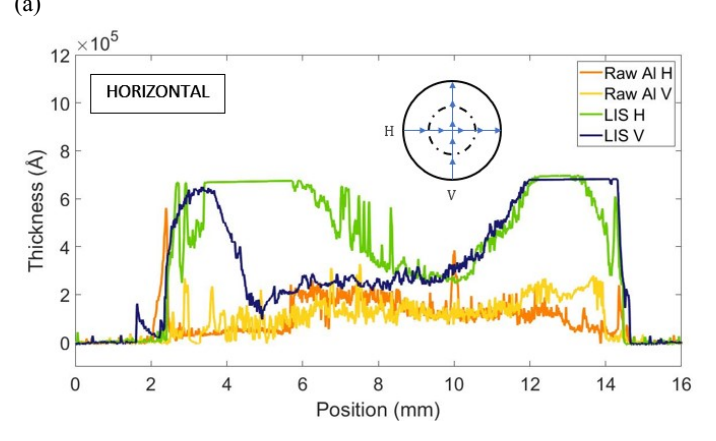


FIGURE 3: Normalized BHTC over 7.5 hours at constant heat flux $(1050 \text{ kw/m}^2 \text{ for plain aluminum and } 150 \text{ kW/m}^2 \text{ for LIS})$. Standard error of measured BHTC/BHTC₀ over the ten minute sampling period for each data point is shown for each set.

For all samples we observe a deterioration of the BHTC over time. Over the sampling period, the BHTC of the horizontal plain aluminum sample degraded by $7.0\pm0.9\%$ while the vertical plain aluminum sample degraded by 7.9±0.8%. The horizontal LIS degraded by 5.6±0.7% and the vertical LIS degraded by 5.4±0.8%. Initial wall superheats for the horizontal and vertical plain aluminum sample stabilized at 18.5 K and 19.2 K respectively. While it was predicted that at a heat flux of 150 kW/m² the LIS surface temperature would stabilize to an initial superheat of 18 K, during experiments the initial surface superheat stabilized at values of 3.1 K (horizontal) and 3.5 K (vertical), respectively. We propose that during the transient ramp-up phase to reach thermal equilibrium, the lubricant layer degraded and a nucleate boiling phase appeared on the surface, leading to a sustained heat flux of 150 kW/m² at such a low surface temperature. Indeed, using high-speed imaging, after some time we observe the transition from film to nucleate boiling, which also seems to affect CHF (not shown here). Because the sample still exhibited superhydrophobic properties after nucleate boiling had started, it is probable that the lubricant is responsible for preventing bubbles from leaving the sample surface in the first place (compare to Fig. 2). This also means that the spin coated lubricant layer is very unstable and deteriorates quickly during boiling. The deterioration of the heat transfer performance over time, as shown in Fig. 3, however should be attributed to the built-up of salt during the experiments.

To quantify the amount of scale built-up during the 7.5 hour BHTC experiments, profilometry was used to measure the thickness of the CaSO4 layer. In order to maintain the CaSO4 layer on the samples, a conformal layer of parylene (SCS Parylene Deposition system) was coated on each sample prior to profilometry testing. Once the coating was applied, each sample was scanned using a KLA-Tencor Alpha-Step D-100 profilometer. The samples were scanned in two perpendicular directions using a 16 mm scan length and a needle force of 1.0 mg. Three scans were taken in each direction and their data were averaged to obtain the results shown in Fig. 4.



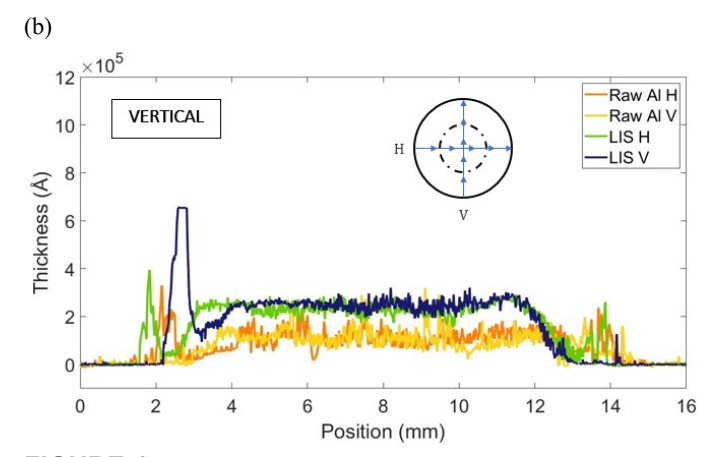


FIGURE 4: Scaling thickness after 7.5 hours at constant heat flux. A diagram of the sample is superimposed on each graph. The surface of interest is enclosed within the dashed lines and two randomly chosen perpendicular needle paths are labeled as H and V. (a) Sample surface horizontally oriented. (b) Sample surface vertically oriented.

In all cases, the LIS developed a thicker layer of salt than the plain aluminum after the 7.5-hour run. Initially, the existence of the lubricant reduces the nucleation rate of salt deposits¹¹. Crystallization develops along the receding inner boundary during bubble departure¹². For LIS, the initial absence of nucleate boiling and bubble departure prevents the deposition of salt. Lubricant infused surfaces have also been shown to lower salt adhesion, a characteristic that wasn't quantified in these experiments⁷. However, as the surface deteriorates and the lubricant drains, the bubble nucleation rate increases, and so does the salt deposition rate. As the heat flux in the long-run experiments on LIS was lower than on the plain surface, we would have expected a lower deposit thickness. The reason for the enhanced deposition is yet to be determined. As can be seen in Fig. 4, the salt layer is especially thick close to the edges of the sample. Deposition was expected to be concentrated somewhat close to the edges of the sample due to confinement effects. However, variation in deposit thickness were particularly pronounced on the LIS sample, as seen from the remarkably different vellow and purple curves in Fig. 4. It is possible that a chip of the salt layer was removed from the surface during boiling, causing the pronounced cavity towards the center of the sample. There was no significant difference in salt deposition between the plain aluminum surfaces in either orientation. As expected due to buoyancy effects, the average deposit thickness was higher on the horizontal sample (18 µm) compared to the vertical orientation (12 µm). For both orientations, the plain aluminum surface outperformed the LIS in minimizing the thickness of salt deposition in the long-run, meaning a plain, vertical surface performs best, contrary to our initial hypothesis.

The scaling thickness on the LIS was greater than the thickness on the plain aluminum surfaces. Scaling measurements in past investigations have used the mass gain analysis instead of profilometry to quantify scaling¹². Quantifying scaling using both methods would also inform on the density of the crystal layer as a factor for BHTC evolution. The CaSO₄ layer is a

porous microstructure that influences surface wettability. Surfaces fabricated with micropillars have been shown to delay onset of film boiling and increase CHF by guiding liquid through the microstructure via capillary wicking¹³. A nondimensional grouping of CHF, latent heat, surface tension, vapor density, liquid density, and gravitational acceleration was proposed by Kutateladze to predict CHF¹⁴. A modification of that coefficient was proposed by Rahman et al. to describe the difference between wicking and non-wicking surfaces based on achieved volumetric flux of liquid through surface microstructures¹⁵. Based on preliminary experiments, we also observe an increase in CHF for both sample types and orientations as scaling progresses. Future work will need to address the physics behind LIS deterioration and quantify heat flux curves for long-run boiling experiments on LIS and plain aluminum surfaces to identify CHF and BHTC across a spectrum of superheats. A useful elaboration of these experiments would be to quantify the porosity of the calcium sulfate layer and apply the proposed model by Rahman et al. to explain potential disparities in CHF for LIS and plain surfaces.

4. CONCLUSION

In an effort to decrease scaling and the accompanying deterioration in heat transfer performance, we compared the boiling behavior for plain aluminum surfaces and lubricant infused surfaces in a horizontal and vertical orientation during pool boiling in salt water. Surprisingly, the thickness of the salt deposition was higher on the LIS than on the plain surface. Yet the heat transfer coefficient decreased less on the LIS during a 7.5-hour boiling experiment. Currently, the insights on the underlying mechanisms are inconclusive, and further investigations are necessary to elucidate the influence of the lubricant on pool boiling heat transfer and fouling.

ACKNOWLEDGEMENTS

The authors acknowledge financial support from Washington University in St. Louis and the Institute of Materials Science and Engineering for the use of instruments and staff assistance. This material is based upon work supported by the National Science Foundation under Grant No. 1856722.

REFERENCES

- [1] Kim, Jinsub; Jun, Seongchul; Lee, Jungho; Godinez, Juan; You, Seung M. *Journal of Heat Transfer*, 2017
- [2] Dash, Susmita; Rapoport, Leonid; Varanasi, Kripa K. *Langmuir*, 2018
- [3] Cai, Yongwei; Liu, Mingyan; Hui, Longfei. *Ind. Eng. Chem. Res.*, 2014
- [4] Bornhorst, Antje; Müller-Steinhagen, Hans; Zhao, Qi. *Heat Transfer Engineering*, 2009
- [5] Wong, Tak-Sing; Kang, Sung Hoon; Tang, Sindy K. Y.; Smythe, Elizabeth J.; Hatton, Benjamin D.; Grinthal, Alison; Aizenberg, Joanna. *Nature*, 2011
- [6] Solomon, Brian R.; Subramanyam, Srinivas B.; Farnham, Taylor A.; Khalil, Karim S.; Anand, Sushnat; Varanasi,

- Kripa K. Non-Wettable Surf., Royal Society of Chemistry, Camridge, 2016
- [7] Anand, Sushant; Paxson, Adam T.; Dhiman, Rajeev; Smith, J. David; Varanasi, Kripa K. *ACS Nano*, 2012
- [8] Weisensee, Patricia B.; Wang, Yunbo; Qian Hongliang; Schultz, Daniel; King, William P.; Milijkovic, Nenad. *International Journal of Heat and Mass Transfer*, 2017
- [9] Wei, Cunqian; Zhang, Guangfa; Zhang, Qinghua; Zhan, Xiaoli; Chen, Fengqiu. *ACS Appl. Mater. Interfaces*, 2016
- [10] Amini, Shahrouz; Kolle, Stefan; Petrone, Luigi; Ahanotu, Onyemaechi; Sunny, Steffi; Sutanto, Clarinda N.; Hoon, Shawn; Cohen, Lucas; Weaver, James C.; Aizenberg, Joanna; Vogel, Nicolas; Miserez, Ali. *Science*, 2017
- [11] Malayeri, M. R.; Al-Janabi, A.; Müller-Steinhagen, H. *Int. J. Energy Res.* 2009
- [12] Subramanyam, Srinivas B.; Azimi, Gisele; Varanasi, Kripa K. *Adv. Mater. Interfaces*, 2014
- [13] Rahman, M.; Ölçeroglu, E.; McCarthy, M. *Langmuir*, 2014
- [14] Kutateladze, S. S. *Izvestia Akademia Nauk, S.S.S.R.*, *Otdelenie Tekhnicheski Nauk*, 1951
 - [15] Zuber, Novak. University of California, 1959